Journal of Power and Energy Engineering, 2025, 13(9), 371-401
https://www.scirp.org/journal/jpee
ISSN Online: 2327-5901
ISSN Print: 2327-588X

Optimal Analysis and Performance of Rwandan Electrical Network with High Penetration of Interconnected PV Rooftop Microgrids

Emmanuel Nisingizwe[1,2*], Mahamat Adoum Abdoulaye[3,4], Cyrus W. Wekesa[1,5], Michael J. Saulo[1,6]

[1]Department of Electrical Engineering, Pan African University Institute for Basic Sciences, Technology and Innovation, Nairobi, Kenya
[2]Department of Environmental Management and Renewable Energy, University of Technology and Arts of Byumba (UTAB), Gicumbi, Rwanda
[3]Department of Physics, University of Nairobi, Nairobi, Kenya
[4]Distributed Energy Team, Jeju Global Research Center, Korea Institute of Energy Research, Jeju, Korea
[5]School of Engineering, University of Eldoret, Eldoret, Kenya
[6]School of Engineering and Technology, Technical University of Mombasa, Mombasa, Kenya
Email: *nisingizwee@gmail.com

How to cite this paper: Nisingizwe, E., Abdoulaye, M.A., Wekesa, C.W. and Saulo, M.J. (2025) Optimal Analysis and Performance of Rwandan Electrical Network with High Penetration of Interconnected PV Rooftop Microgrids. *Journal of Power and Energy Engineering*, **13**, 371-401.
https://doi.org/10.4236/jpee.2025.139024

Received: August 3, 2025
Accepted: September 23, 2025
Published: September 26, 2025

Copyright © 2025 by author(s) and Scientific Research Publishing Inc.
This work is licensed under the Creative Commons Attribution-NonCommercial International License (CC BY-NC 4.0).
http://creativecommons.org/licenses/by-nc/4.0/
Open Access

Abstract

This study investigates the optimal integration and performance of interconnected rooftop photovoltaic (PV) microgrids within Rwanda's electrical distribution network, supporting the nation's goals for widespread electrification and renewable energy adoption. Through a detailed case study, the research addresses technical, economic, operational, social, and environmental challenges associated with high PV microgrid penetration. Advanced simulations conducted using MATLAB evaluate the system's performance across various scenarios, focusing on voltage stability, power quality, and energy losses. The findings reveal that interconnected microgrids significantly enhance network resilience, energy access, and renewable energy integration, particularly in remote areas. Key technical results demonstrate a robust and efficient system, with a System Self-Sufficiency Index (SSSI) of 0.4186, a System Self-Consumption Index (SSCI) of 0.3088, an excess energy generation of 3568803.59 kWh, zero unmet load, a very low Loss of Power Supply Probability (LPSP) of 0.0096, and a total energy transfer of 3913515.11 kWh. Economic analysis highlights strong financial viability, with a low Levelized Cost of Energy (LCOE) of $0.04/kWh, a Net Present Cost (NPC) of $8867793.27, and a payback period of 9.6 years. Socially, the optimized systems are expected to create three direct jobs per installation, improve the Human Development Index (HDI), and achieve high social acceptance, supported by a 95% positive response rate toward renewable energy adoption. Environmentally, the systems avoid 10374932.8 kilograms of

CO_2 emissions and achieve a remarkable renewable energy penetration rate of 97.75%. Overall, this study demonstrates the technical, economic, social, and environmental benefits of high PV microgrid penetration in Rwanda and provides actionable insights for policymakers, engineers, and stakeholders aiming to maximize the advantages of microgrid integration while addressing associated challenges.

Keywords

Rooftop PV Microgrids, Battery Storage, Electrical Distribution Networks, Evaluation Criteria, Energy Management

1. Introduction

1.1. Background and Literature Review

The International Energy Agency's assessment finds that carbon emissions and electricity demand might rise by 70% and 65%, respectively, during the next 20 years if appropriate measures are not taken [1]. Approximately 40% of electricity consumption is attributed to the residential and commercial edifice sectors [2]. Incorporating renewable energy has been a critical emphasis for environmental advocates and legislators in an effort to lower electricity usage and carbon output through the frequent use of PV systems for residential homes [3]. Installing PV systems on rooftops helps lower emissions and reduce electricity costs [4]. Additionally, the shift toward sustainable energy has increased interest in decentralized solutions, particularly in regions with underdeveloped energy infrastructure, such as sub-Saharan Africa, including Rwanda. Renewable energy-based microgrids improve local energy resilience and have emerged as a vital part of this transition [5].

The global energy sector must achieve one of the Sustainable Development Goal's which is cleaner technologies by accessing modern, affordable, sustainable, and dependable energy by 2030 [6]. In order to track the progress towards the "Net Zero Scenario by 2050", the share of renewable energy in the power grid must rise by 13% per year until 2030, when it will account for 60% of total generation [7]. A substantial shift in the global energy framework towards cleaner technologies is necessary to meet the Sustainable Development Goal of "providing access to affordable, reliable, sustainable, and modern energy for everyone by 2030" Incorporating various energy sources into the grid requires efficient storage options to handle surplus renewable output and provide electricity during times of low generation. Nonetheless, the widespread implementation of energy storage systems brings about complexities and extra expenses [8].

Power losses in photovoltaic (PV) systems arise from various factors, including inefficiencies in system components, mismatched panel characteristics, shading, contamination, and increased PV penetration levels [9]. One approach to mitigat-

ing these losses is the integration of Distributed Generation (DG). Proper positioning and sizing of DG are crucial, as improper implementation can lead to feeder overload and further power losses. If PV generation exceeds consumer demand, surplus produced energy is fed back into the network, altering feeder currents [10]. High levels of PV penetration can further amplify these current fluctuations, aggravating power losses. To address these challenges, a voltage and demand management method has been studied in [11], significantly enhancing distribution networks' capacity to accommodate and utilize PV generation for distributed battery storage. In [12], researchers investigated the impact of increasing PV's penetration on distribution load tap changer operations. They included steady-state and quasi-static power flow experiments in their study, which was based on simulations of two distribution feeder circuits. The findings showed that when penetration reached 30% or more, generating voltage oscillations, the tap change position significantly increased. Future studies are encouraged to confirm and improve system performance by integrating an adaptive HVAC control technique into quasi-static power flow analysis in order to lessen these effects.

There are related power losses effects and studies related to 1 MWp of installed rooftop solar system at the Kaohsiung World Games Stadium, as well as without it. To improve the precision of PV power generation modeling, the authors integrated real-time measurements of various parameters of that PV system such as solar radiation, temperature, etc. Different strategies have been suggested to minimize the system losses; these strategies are such as a multi-objective Optimal Power Flow (OPF) method [13] and a refined reference scheduling technique. In [14], research was carried out on a highly unstable radial Low Voltage (LV) distribution network under elevated PV penetration levels on a summer day. The findings showed differences in power losses among various testing methods, with self-consumption and storage modes recognized as the most efficient strategies. To enhance the incorporation of high levels of renewable energy, [15] proposed a machine learning (ML) oriented method. The creation of control frameworks may aid in decreasing communication needs, whereas certain peer-to-peer energy trading systems guarantee minimal latency and alignment with data sharing. These results can help in creating localized renewable energy generation and storage systems that minimize voltage drops, efficiently satisfying local energy needs. Future developments in intelligent inverters for high-penetration rooftop solar installations are anticipated to improve efficiency and decrease device dimensions. Moreover, it is expected that interoperability and communication protocols will grow through ML algorithms. A framework for evaluating voltage stability in power networks featuring PV systems and variable loads was presented by [16]. This method utilizes a Monte Carlo Simulation to consider the fluctuations and unpredictability of PV energy sources and system requirements. Results indicate that with rising PV penetration, total system line losses diminish, and the reactive power margin at the load bus is enhanced, especially during solar irradiation's peak hours.

A study examining the effects of rooftop solar systems by [17] on power generation systems is not an established approach for forecasting the secure level of solar integration for transmission networks. The permissible penetration level is established by the feeder configuration, load characteristics, and solar/cloud dynamics during the day. The upper limit for solar input is identified as the moment when voltage rises and/or flicker issues start to happen. Regardless of comparable penetration levels and weather conditions, the design of the feeder influences the threshold. Accurate information is just as important in assessing the permissible level of solar power integration. However, the Rooftop Solar PV installation results in reduced operating costs. There are issues with inefficiency, and it is additionally untrustworthy. In [18], the authors introduced a method for scheduling energy consumption that self-regulates, aimed at reducing the peak load from large rooftop PV installations and lowering RPF. They created stochastic programming due to the inconsistent power generation from PV. The proposed algorithm might alleviate the voltage rise problem and the peak-to-average ratio of the overall load. The primary problem resulting from RPF is a rise in voltage. When the electricity generated by PV exceeds user demand, the voltage at the inverter's Point of Common Coupling with the grid increases. Reducing the elevated voltage in the network is the most effective way to mitigate the negative impacts of high PV levels.

Power quality issues arise from fluctuations in renewable systems, which are frequently brought on by bad weather or connectivity issues. [19] has offered an experimental investigation that uses a cloud shadow technique to address technical problems such as voltage and power variations. According to the modelling results, variations may be managed at 50% PV penetration levels. Voltage fluctuations can interfere with the production of power, damaging system components and perhaps costing the system owner money and lowering energy output [20]. Because LV feeders are typically situated a considerable distance from the main substation and frequently exhibit low power or failure rates, they may result in voltage variations at the output of the solar panel [21]. Notable rises in the installation of rooftop PV systems cause issues like voltage imbalance, affecting the grid's power quality. Voltage unbalance arises from unpredictable current and impedance linked to the disparity between net demand and net generation, and it often worsens due to the uneven arrangement of PV panels. The quality of power is greatly influenced by the frequency. A change in the load results in frequency alterations within the grid, and the frequency is also affected as the active power from the PV output varies with solar radiation [22]. The real power could increase due to the drop in frequency caused by generation losses and a higher load. Furthermore, generator emulation controls accomplish this by instructing the inverter to reduce the real power output as the line frequency rises. When energy usage is elevated, the demand for energy rises, resulting in a further decline in frequency. Grid-tied PV systems need a consistent frequency for effective functioning, and the inverter should not exceed a frequency error of 2% [23].

1.2. Research Gaps and Study Objectives

While earlier studies offer important perspectives on renewable energy across various regions, limited research has been carried out to integrate technical, economic, and social models tailored to the ideal design of rooftop PV implementation in Western Rwanda's Rwamagana District, particularly as this region is rapidly advancing in industrialization and e-mobility being one of the closest districts to Kigali City. Moreover, the viability from a techno-economic standpoint is already well understood. Thus, this manuscript, Optimal Analysis and Performance of Electrical Network with High Penetration of Interconnected PV Rooftop Microgrids: Case Study of Rwanda, explores the issues and possibilities linked to the extensive implementation of interconnected PV microgrids in Rwanda's electrical distribution network. Rwanda serves as a compelling case study because of its bold electrification objectives, which encompass a notable rise in e-transportation and industrial development. Therefore, depending on distributed renewable energy systems to meet these goals may be an optimal solution. The paper examines the technical, operational, and planning consequences of incorporating a high level of rooftop PV microgrids into the national grid. By examining the Rwandan context, the research offers perspectives on optimizing interconnected rooftop PV microgrids to tackle issues like voltage regulation, load balancing, and power reliability in both rural and urban environments.

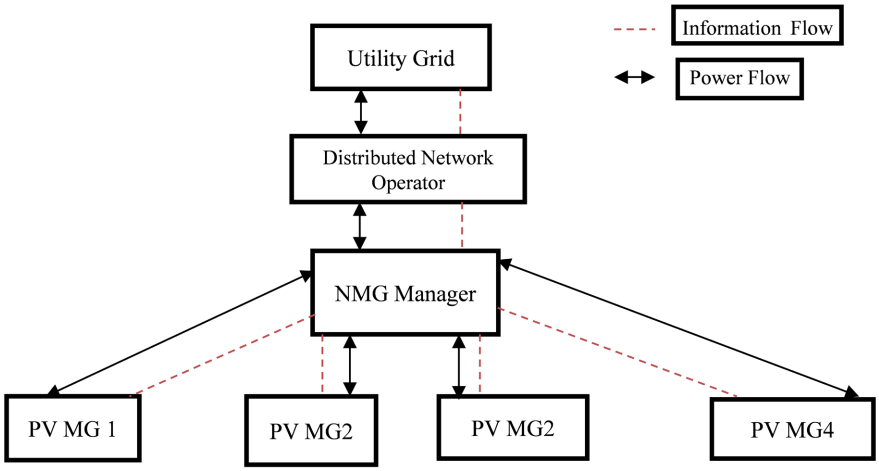

Figure 1. Model of proposed networked PV microgrids.

The study utilizes sophisticated modeling methods with MATLAB and PSO to emulate network efficiency across diverse microgrid penetration situations, providing a framework for analogous uses in additional developing countries. Moreover, the research highlights the significance of regulatory structures, updates to grid codes, and investment approaches that facilitate the cohabitation of centralized and decentralized energy systems. In conclusion, this paper adds to the wider discussion on how linked microgrids can transform energy access, especially in areas with limited resources, by thoroughly examining their effects on electrical distri-

bution systems in Rwanda. The primary contributions to this article consist of:

- Evaluate the technical effects of interconnected rooftop PV microgrids on voltage stability, power losses, and network dependability.
- Assess the suitability of the current distribution network framework for decentralized energy production.
- Suggest approaches for enhancing the integration of rooftop PV microgrids to reduce interruptions and increase efficiency as shown in Figure 1.

2. Methodology

The research methods employed to accomplish the stated goals are described in depth in this section. The methodology describes the study area and load characteristics, the hybrid renewable energy systems that are analysed and their component modelling, the optimisation technique, the evaluation of the objective functions, the techno-economic aspects of the system, and the suggested energy and storage management framework.

2.1. Study Location and Load Profile

The study was conducted at the Rwamagana Industrial Park, which is part of the eastern network that includes the districts of Nyagatare, Kayonza, Ngoma, Kirehe, Gatsibo, and Rwamagana. The coordinates of this location are 30.4386˚E and 1.9535˚S. A Rwamagana feeder with a conductor size of ACSR 70/12 mm^2, a maximum power capacity of 12.05 MW, and a peak output of 2.2 MW supplies the research area. A 110/15 kV, 10 MVA power transformer steps down the 110 kV voltage level.

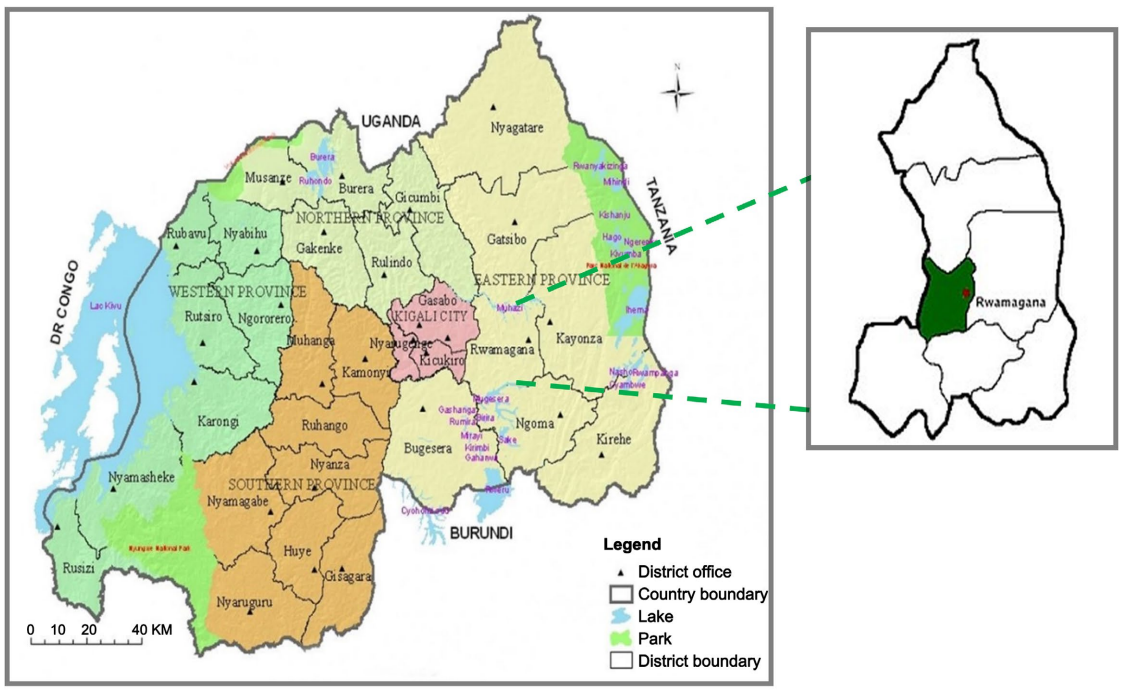

Figure 2. Geographical location of Rwamagana, Rwanda.

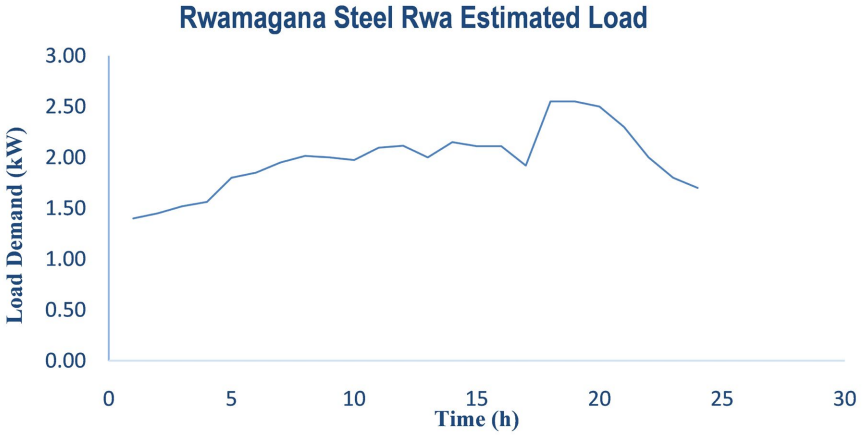

Figure 3. Rwamagana Steel Rwa hourly load variation in a day.

Critical projects that need sufficient electricity to run enterprises, such as irrigation, milk collection centres, mining, and special economic zones in the districts of Nyagatare and Rwamagana, are being carried out in the study region as shown in Figure 2. Hourly demand fluctuated significantly during the year, as was to be expected. With the exception of blackouts, the lowest recorded load was roughly 1.45 kW, while the highest recorded load was 2.5 kW. As seen in Figure 3, the connected load consistently stays rather high between 18:00 and 21:00, peaking at about 19:00 (Figure 4).

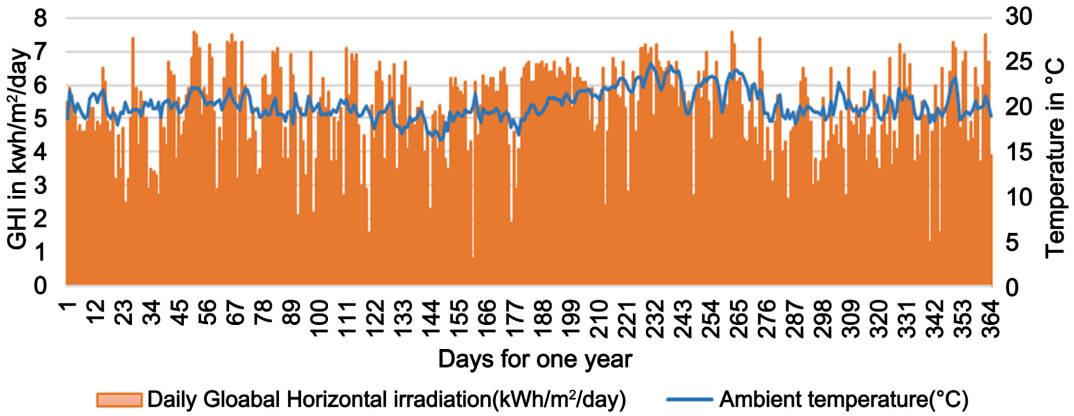

Figure 4. Daily meteorology data for Rwamagana Industrial Park over a year.

2.2. Renewable Energy Systems Configuration and Modeling

This section outlines the topology of connected rooftop PV networked microgrids (NMG) examined in this research and discusses the modeling of different components, including PV, BESS, grid, and loads of each microgrid within the connected system.

2.2.1. PV NMG System Configuration

The configuration under consideration is illustrated in Figure 5, considering prosumers with residential, commercial, and industrial loads, respectively. Com-

mercial and industrial structures offer ample space for a large rooftop PV array, leading to greater electricity generation capacity, while residential buildings provide less room. The electricity produced by PV meets the local load demand and, once satisfied, transmits any excess electricity to the grid. When the PV generation falls short of the demand, the grid provides the necessary electricity to meet the loads.

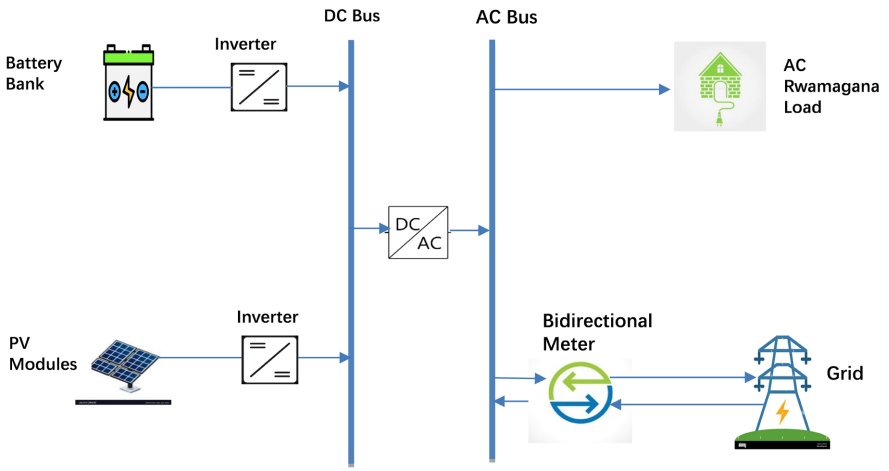

Figure 5. Proposed system configuration. Grid-PV-Battery.

2.2.2. Grid-PV-Battery System Modeling

Three setups are assessed for their technical, economic, environmental, and social aspects to deliver electricity to the analyzed region. In this part, we address the modeling of Grid, PV, and BESS for every microgrid (MG) within a networked structure. Three scenarios are also examined, which include: Grid-PV-BESS-Load, Grid-PV-Load, and PV-BESS-Load. This suggested system can facilitate a two-way power flow with the grid, either acquiring or supplying electricity.

A) Photovoltaic Panel Modeling

The hourly power output of the photovoltaic panels, referred to as PPV (kW), is determined by Equation (1) and is influenced by solar irradiation and ambient temperature [24] [25].

$$P_{pv} = N_{pv} \times X_{pv} f_{pv} \times \frac{S_T}{S_{T,STC}} \times \left[1 + \alpha_P \left(T_C - T_{C,STC}\right)\right] \quad (1)$$

The variables relevant to this context include N_{pv}, which represents the total number of photovoltaic panels; X_{pv}, the rated power output of the PV system in kilowatts; and f_{pv}, the derating factor given as a percentage. S_T stands for the total irradiance on the tilted PV surface, measured in kW/m^2; while $S_{T,STC}$ refers to the standard solar irradiance value of 1 kW/m^2. The symbol α_P, represents the power temperature coefficient in percentage per degree Celsius (%/˚C). Additionally, T_C is the PV cell temperature in degrees Celsius, and $T_{C,STC}$ denotes the cell temperature under normal conditions.

B) Battery Storage System Modeling

Battery storage systems function as backup energy reservoirs when the electricity generated by RE sources falls short of fulfilling the demand [26]. The batteries are recharged when the PV generator generates enough electricity to fulfill requirements and are drained when their production is inadequate to satisfy consumption needs. Consequently, they are essential for the proper operation of a hybrid system. The flowcharts in **Figure 5** illustrate the equations that depict battery functioning (both charging and discharging), where it is incorporated. [27] indicate that the subsequent restrictions influence the manner in which the battery's energy may be stored:

$$\begin{cases} E_{b,\min} \le E_b(t) \le E_{b,\max} \\ E_{b,\max} = N_b E_{b,cap} \\ E_{b,\min} = E_{b,\max}(1-\mathrm{DOD}) \end{cases} \tag{2}$$

Here, N_b denotes the total number of batteries, $E_{b,\max}$ (kWh) signifies the highest necessary storage battery capacity, $E_{b,\min}$ (kWh) refers to the minimum permissible storage battery capacity, and $E_{b,cap}$ represents the battery's nominal capacity (kWh). DOD indicates the depth to which the battery has been discharged.

C) Inverter Modeling

As stated in [28], Equation (3) specifies the dimensions of the inverter (P_{inv}) in a hybrid RE setup. [29] clarified this equation, indicating that the inverter needs to possess a capacity 8% - 10% greater than the power demand for assuring safety.

$$P_{inv} = \frac{P_{peak}}{\mu_{inv}} \tag{3}$$

D) Grid Modeling

The national grid delivers interrupted electricity to the system. When the PV-Wind-BES system does not have enough power to meet demand, this equation calculates the electricity received from the grid [30].

$$P_g = P_l(t) - \left\{P_{pv}(t) + P_w(t) + P_b(t)\right\} \tag{4}$$

where P_g, $P_l(t)$, $P_{pv}(t)$, $P_w(t)$, $P_b(t)$ are the power compensated by the grid, load connected, PV-module output power, wind turbine's generated power (kW), and power stored in BES respectively.

2.3. Grid-Connected Microgrid

Energy management approaches need to be applied as the microgrid is linked to the grid. The microgrid needs to facilitate energy trading, enabling it to sell excess generation or draw energy from the grid in times of shortage. Equation (5) illustrates the approach for determining the objective function to reduce the operating costs of the interconnected microgrid. The objective function considers the expenses of the generating units.

$$\min \sum_{t=1}^{24} C_{MG}(t) P(t) \tag{5}$$

where:

C_{MG} represents the expense for each generation unit.

$P(t)$ is DG-generated power.

$C_{MG}(t)$ represents the cost for each unit of controllable produced power.

MG represents the produced energy for each unit and the sold power to the grid.

2.4. Energy Management System

To effectively control the power flow and accomplish the goal function by specifying decision variables, the optimisation system must be implemented in the microgrid's energy management relationship. The ideal power flow in this study aims to lower MG's operating costs while increasing the utilisation of renewables. Equation (6) [31] can be used to characterise the target function for every time interval:

$$\min \sum_{t=1}^{T} P_{pv}(t) C_{pv} + P_{storage}(t) C_{storage} + P_{grid}(t) C_{grid} \tag{6}$$

Here, P_{pv} & $P_{storage}$ denote the supplied power from PV and storage generation, respectively.

C_{pv} & $C_{storage}$ denote respectively the costs related to the operation and maintenance of generated power from the PV and storage.

C_{grid} denotes electricity cost from the grid during period *t*.

T indicates the overall time of optimization, which is a daily range.

In order to address the optimisation system and its objective function, constraints must be considered. Equation (7) can be used to express the power balance constraint of the system.

$$\sum P_{load}(t) P_{pv}(t) - P_{storage}(t) P_{grid} = 0 \tag{7}$$

where:

P_{load} is the total consumed power of the microgrid.

The P_{pv} & $P_{storage}$ should be capped to ensure system stability; these parameters are restricted to predetermined maximum PV and BESS values, along with upholding defined SOC's maximum and minimum levels of BESS as outlined in Equations (8) & (9).

$$\begin{cases} P_{pv}^{\min} \le P_{pv} \le P_{pv}^{\max} \\ P_{storage}^{\min} \le P_{storage} \le P_{storage}^{\max} \end{cases} \tag{8}$$

$$\begin{cases} \mathrm{SOC}_{\min} \le \mathrm{SOC} \le \mathrm{SOC}_{\max} \\ E_{storage}^{\min} \le E_{storage} \le E_{storage}^{\max} \end{cases} \tag{9}$$

where:

E is the BESS capacity.

It is equally important to take into account the constraints linked to energy indicators described in Equations (11) and (12), which illustrate how the energy management in the electricity lab will result in a decrease in consumption per area

and per user.

$$\frac{Users}{Load} < P_{MG} \tag{10}$$

$$\frac{Area}{Load} < P_{MG} \tag{11}$$

where:

Users refer to the count of individuals operating within the microgrid.

Load refers to the demand needed at the meter boundary with the utility.

Area represents the covered area by the microgrid about the energy demand needed at the utility boundary meter.

The balance of the power consumption, provision, and charging process of the battery is very important in this study, while minimizing NPC and maximizing reliability. Therefore, the control and the fundamental concepts of the suggested operational strategies are outlined as follows:

A) PV-Grid-Storage-Load:

Following the maximum export power threshold ($P_e^{\max}$), surplus energy is sent to the main grid if PV system's power generation (P_{pv}) surpasses the household's consumption (P_l).

$$P_e(t) = \min\left(P_e^{\max}, P_{pv}(t) - P_l(t)\right) \tag{12}$$

$$P_{pv}(t) = N_{pv} * P_{pv}^{rated}(t) \tag{13}$$

The solar PV system's inverter is used to redirect extra power if the export power exceeds the limit. The expression for the discarded energy (P_d) is:

$$P_d(t) = P_{pv}(t) - P_l(t) - P_e^{\max} \tag{14}$$

B) PV-Grid-Load:

If P_{pv} is below the load, then the shortage of power is acquired from the grid.

$$P_i(t) = P_l(t) - P_{pv}(t) \tag{15}$$

And then, by exporting the maximum power to the grid, the extra power of PV is dumped.

$$P_d(t) = P_{pv}(t) - P_l(t) - P_e^{\max} \tag{16}$$

C) PV-BESS-Load:

If the BES has charge available, it will be discharged to provide the required amount of power.

$$P_b^{disch}(t) = P_l(t) - P_{pv}(t) \tag{17}$$

If the initial condition isn't satisfied and the leftover load does not exceed the battery's input, then any surplus power from the PV charges the battery:

$$P_b^{ch}(t) = P_{pv}(t) - P_l(t) \tag{18}$$

The below equations used to determine the battery's SOC level and available input and output power restrictions at each time interval:

$$P_b^{in}(t) = \min\left(P_b^{\max}, (E_b/\Delta t) * \left(\mathrm{SOC}_b^{\max} - \mathrm{SOC}_b(t)\right)\right) \quad (19)$$

$$P_b^{out}(t) = \min\left(P_b^{\max}, (E_b/\Delta t) * \left(\mathrm{SOC}_b(t) - \mathrm{SOC}_b^{\min}\right)\right) \quad (20)$$

$$\mathrm{SOC}_b(t+\Delta t) = \mathrm{SOC}_b(t) + \frac{P_b^{ch}(t) * \eta_b^{ch} - \frac{P_b^{disch}(t)}{\eta_b^{disch}}}{\frac{E_b^{\max}}{\Delta t}} \quad (21)$$

3. Optimization and Criteria Evaluation

This section describes the optimisation model that was used to size the PV and BES. This includes the evaluation criteria, design restrictions, objective function, and optimisation approach.

3.1. Optimization Approach

Three configurations of the hybrid system (PV-Grid-Storage, PV-Grid, and PV-BESS) will be evaluated techno-economically, environmentally, and socially in this study using MOPSO, a heuristic method modelled after the social dynamics

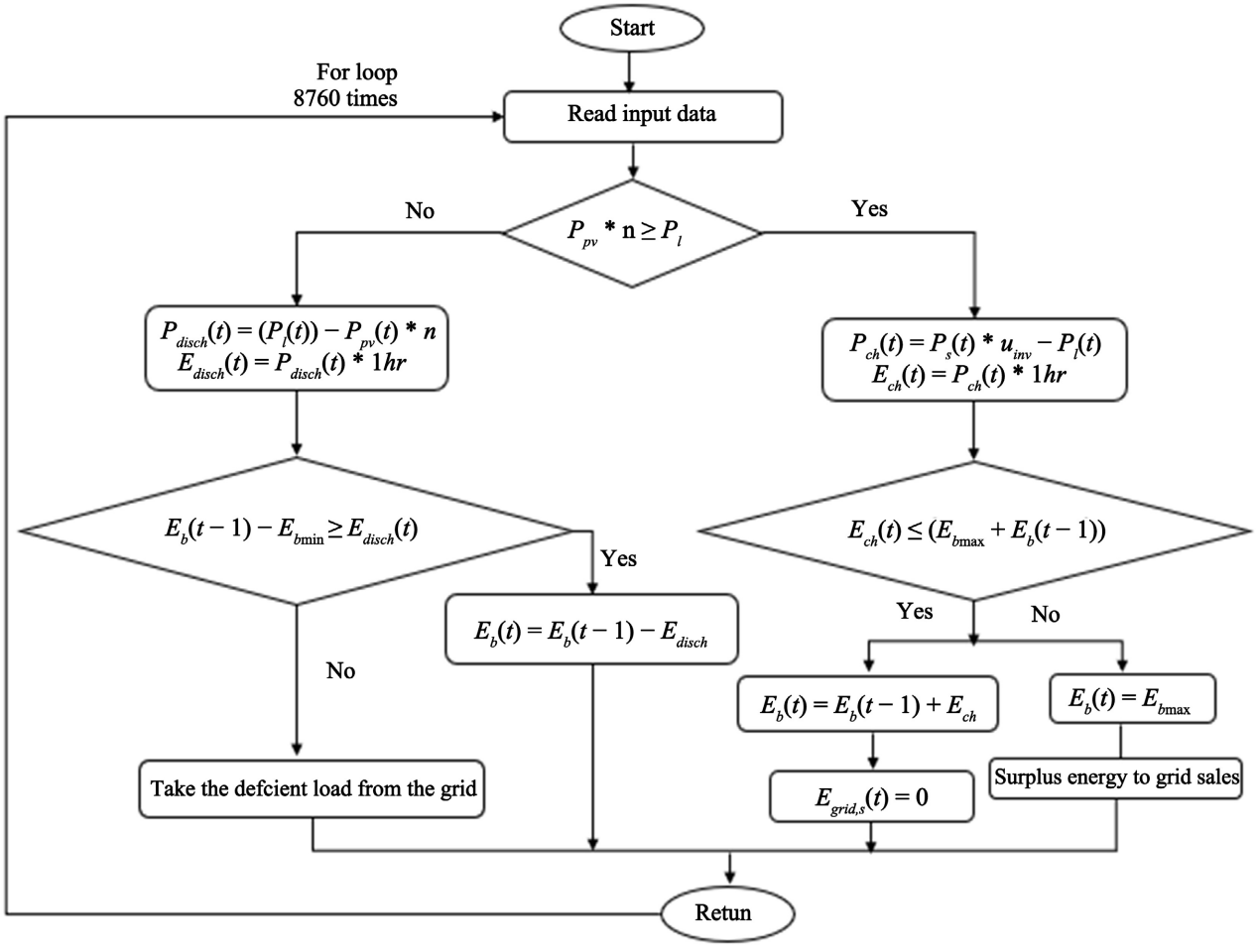

Figure 6. Flowchart for the energy management of proposed system.

of a flock of birds [32]. This is a straightforward approach that depends on the populace. Every particle in PSO represents a possible fix for the issue at hand. To get the best results, the particles in PSO move around in the high-dimensional search space and change their positions. In PSO, every particle is linked to both its own optimal location and the overall optimal position for all particles. The trajectory of these particles depends on each particle's velocity, influenced by its own best performance, highest performance of others, reflecting the individual travel experience of the particle and the experiences of neighboring particles [33]. MOPSO replaces PSO for Single Objective Functions: Unlike PSO, in which all objective functions share a common neighborhood, MOPSO allows each function to keep its distinct area for position updates. The update for velocity in MOPSO is presented in Equation (22). The mutation operator is utilized to enhance the diversity of the quest to achieve the ideal solution.

The particles that perform best for each objective function are kept in an external archive known as the repository (REP)

$$v_i^t = w * v_i^{t-1} + c_1 * rand(\,) * \left(x_{Pbest_i} - x_i^t\right) + c_2 * Rand(\,) * \left(\mathrm{REP}_{(h)} - x_i^t\right). \quad (22)$$

The value $\mathrm{REP}_{(h)}$ is taken from the repository. **Figure 6** illustrates the detailed process for minimising the AEC and LPSP problems as employing MOPSO.

3.2. Design Constraints

The following equations illustrate the design limitations of the optimization issue:

$$0 \le P_{pv}(t) \le P_{pv}^{\max} \quad (23)$$

$$0 \le P_{storage}^{ch}(t), P_{storage}^{disch}(t) \le P_{storage}^{\max} \quad (24)$$

$$\mathrm{SOC}_{storage}^{\min} \le \mathrm{SOC}_{storage}(t) \le \mathrm{SOC}_{storage}^{\max} \quad (25)$$

$$P_{pv}(t) + P_{storage}(t) + P_{imp}(t) - P_{exp}(t) \ge P_d(t) \quad (26)$$

$$0 \le P_{exp}(t) \le P_{exp}^{\max} \quad (27)$$

Equations (23)-(27) represent the power limitations of the PV and BES, respectively. It is important to note that the house's load cannot be controlled. The battery's SOC constraints are specified by Equations (24) and (25), respectively. Equation (26) represents the balance constraint, while Equation (27) indicates exported power limitation from the house's solar PV system to main grid. The restrictions must be applicable for the overall "*t*", which is 8760 hours. Pe represents the power that is exported,

3.3. Evaluation Criteria

Various distinct domain characteristics are used as the basis for selecting the best MG. NPC and COE factors are examined in the economic evaluation. The technical requirements address the unmet load (UL), excess or surplus energy (EE), size, and renewable dispersion (RD). CO_2 as an environmental element is also assessed. Social analysis assesses acceptance in the community and human progress.

When assessing reliability, both availability index and loss of power supply probability abbreviated as AI and LPSP, respectively, are estimated. While COE and NPC are lowered in the economic side, CO and APM are environmentally reduced, and for reliability, the LPSP is decreased.

3.3.1. Technical Criteria

The quantity of energy produced by RES consumed in the MG is determined by the RD factor. This is how RD is computed [31]:

$$\mathrm{RD} = \left(1 - \frac{\sum P_{DG}}{\sum P_{pv} + P_b}\right) \times 100 \tag{28}$$

The annual unfulfilled load divided by the total annual load is known as the UL. This is how UL is determined [34]

$$\mathrm{UL} = \frac{\text{Yearly unfulfilled load}}{\text{Total yearly load}} \tag{29}$$

The further generated energy by the system that is not promptly utilized by connected loads referred as EE in an MG system. Batteries may be used to store this energy, or the energy may be handled by the dump load. EE should be kept to a minimum. This is how EE is computed [31] [34] with values in **Table 1**.

$$\mathrm{EE} = \frac{\sum_{t=1}^{8760}\left(P_{pv}(t) + P_b(t) + P_{bMG} - P_l(t)x\Delta t\right)}{\sum_{t=1}^{8760}\left(P_{pv}(t) + P_b(t) + P_{bMG} + P_{DG}(t)x\Delta t\right)} \tag{30}$$

Table 1. Technical and economic rating of the proposed system components

Components	Ratings	Lifetime
PV module	300 W, 17.2%	25 years
Battery	100 Ah, 12 V	5 years
Inverter	15 kW, 3-phase	10 years
Converter	1 kW	15 years
Project lifespan		25 years
Interest rate	10%	

1) System Self-Sufficiency Index (SSSI)

This criterion evaluates the energy of the system that needs to be fulfilled through its power production instead of depending on external sources like grid electricity. A higher level of SSSI shows increased independence and decreased reliance on outside energy sources. The SSSI measures the percentage of energy coming from RES compared to the overall load demand during a period T [35] [36], as shown in Equation (31). This index can assess the efficiency of multi-energy systems or net-zero energy systems that rely solely on renewable energy sources. Can convert electricity into different forms of energy to meet different energy needs. Additionally, the SSSI can predict energy security and reductions in greenhouse gas emissions.

$$\text{SSSI} = \frac{\int_0^T \min\left\{P_l(t), P_T(t)\right\} \mathrm{d}t}{\int_0^T P_l(t) \mathrm{d}t} \tag{31}$$

2) System Self-Consumption Index (SSCI)

The SSCI evaluates the quantity of energy generated by RES that is utilized internally to fulfil energy demands, instead of being sent back to the grid [37]. A greater Self-Sufficiency Index (SSCI) indicates increased self-reliance and reduced reliance on the electricity grid. SSCI computes the proportion of immediate electricity demand fulfilled by RES compared to the total renewable energy output during a period T [35], as shown in Equation (32).

$$\text{SSCI} = \frac{\int_0^T \min\left\{P_l(t), P_T(t)\right\} \mathrm{d}t}{\int_0^T P_T(t) \mathrm{d}t} \tag{32}$$

3.3.2. Economic Objective Function

The net present cost is computed as follows [38] where NPC is the total of the life's beginning cost (C_{ic}), operation and maintenance costs (C_{om}), and replacement spare costs (C_{rsc}).

$$C_{NPC} = \frac{C_{ic} + C_{rsc} + C_{omc}}{CRF(i_d, t)} \tag{33}$$

$$C_{ic} = \sum N_{com} \times C_{com}; C_{com} = \text{pv, inverter, converter, battery \& DG} \tag{34}$$

$$C_{omc} = \sum N_{com} \times C_{com} \times \sum_{n=1}^{25} \left(\frac{1+i_r}{1+r_r}\right)^n; \quad C_{com} = \text{pv, inverter, converter, battery \& DG} \tag{35}$$

The systems' spare parts for the batteries, DG, inverter, and converter are change, Equation (36) governs the replacement spare costs:

$$C_{rsc} = \sum N_{com} \times C_{com} \times \sum_{n=1}^{25} \left(\frac{i_r}{(1+i_r)^n - 1}\right); \quad C_{com} = \text{pv, inverter, converter, battery \& DG} \tag{36}$$

Equation (37) is used to get capital recovery factor [38]:

$$CRF(i_d, t) = \frac{i_d (1+i_d)^n}{(1+i_d)^n - 1} \tag{37}$$

The cost of electricity per unit, or *COE*, is determined as follows [16]:

$$C_{COE} = \frac{C_{NPC} \times CRF(i_d, t)}{365 \times \sum_{t=1}^{n} P_l(t)} \tag{38}$$

where P_l and n are the load power at time t and the number of years, respectively; r, d, and i stand for interest, annual, and inflation rates, respectively.

3.3.3. Social Parameters

In systems analysis, social influences refer to how the system affects community

and its constituents. This covers elements including safety, dependability, cost-effectiveness, and energy availability. The involvement of stakeholders and the local community in the development, deployment, and supervision of MG systems is another example of a social component. The social component is essential as it guarantees that MG systems are developed then put into place to satisfy community demands and expectations while encouraging sustainable growth.

The creation and upkeep of MGs can lead to employment opportunities in a number of industries, such as engineering, building, installation, and maintenance. There will be a need for qualified experts to plan, develop, and manage these systems as the demand for MGs increases. Additionally, MGs can increase electricity to various industrial zones lacking conventional power sources, opening up employment opportunities in those areas. All things considered, the expansion of MGs can promote sustained economic growth and employment creation. In Rwanda, RESs create new work opportunities. The development of emerging nations is intimately related to expansion of RESs.

Therefore, this is how the job creation opportunity (JCO) is computed and results are presented in **Table 2** [39]:

$$\text{JCO} = \sum JC_{com} \times P_{com}; com = \text{pv, inverter, converter, battery \& DG} \quad (39)$$

where JC_{com} is job creation and P_{com} represents the maximum power of each of system's components.

Human development index (HDI) or socioeconomic development is measured. It also has to do with the energy that people use. The HDI rises in tandem with the energy consumption. This is how the HDI is determined as [40]:

$$\text{HDI} = 0.09788 \log_e \left[\left(E_l + \text{minimize}\left(\varepsilon_{mee} \times E_{ee} \times \varepsilon_{ACl} \times E_l \right) \right) / N_{human} \right] - 0.0310 \varepsilon_{mee} \quad (40)$$

The mechanism appears to link human development to energy-related parameters. Where E_{ee} is the annual EE, ε_{mee} is the factor of EE, E_l is the load energy, and ε_{ACl} is the factor of raising the AC load. where N_{human} is human users' total number of hybrid renewable-energy microgrid systems [31]. The numerator combines the baseline energy with the minimized product of efficiency factors and energy demand, then normalizes by N_{human}, the population. The logarithmic function smooths extreme variations, reflecting diminishing returns of energy access on HDI. This approach emphasizes the role of energy availability and efficiency in shaping human development outcomes such as enabling better access to education or health services through reliable power.

Table 2. Social parameter results.

Job Creation Opportunity (JCO)	3
Human Development Index (HDI)	0.43

3.3.4. Environment Objectives

Avoided carbon dioxide (CO_2) emissions

By choosing to employ renewable energy sources (RES) rather of fossil fuels,

carbon dioxide (CO_2) emissions that are forbidden from entering the atmosphere were avoided. The annual estimate of CO_2 emissions averted by switching from the conventional grid to renewable energy sources is shown in Equation (41) [41].

$$\text{Avoided}_{CO_2} = \left(SO_2 + NO_x + CO_2\right)\left(0.001\right)\left(\sum_{t=1}^{8760} P_{load}\left(t\right) - \sum_{t=1}^{8760} P_{gs}\left(t\right)\right) \quad (41)$$

Using the emission factors for sulphur oxides (SO_x), nitrogen oxides (NO_x), and carbon dioxide (CO_2), as well as a conversion factor of 0.001, the total annual averted CO_2 emissions are calculated in kilogrammes. The amount of greenhouse gas emission reduction brought about by the installation of a grid-connected hybrid system is determined by Equation (42) [42].

$$CO_2 \text{ Saving PV, WT} = \left(\text{PV}_{\text{kWh}} + \text{Bat}_{\text{kWh}}\right) \times 0.747 \frac{\text{kg } CO_2}{\text{kWh}} \quad (42)$$

The system's overall greenhouse gas emissions are determined by multiplying the net grid electricity in kWh by emission factor for each pollutant, which is expressed in g/kWh and are presented in below **Table 3**.

Table 3. Greenhouse gas emission factor [43] [44].

Greenhouse gas	Emission factor value	Unit
SO_2	0.5	gSO_x/kWh
NO_x	0.22	gNO_x/kWh
CO_2	690	gCO_2/kWh

3.3.5. Reliability Objective Index

The reliability index is used to assess the MG's performance. AI and LPSP are crucial dependability measures. LPSP is the shortfall in power generated and delivered to load as a result of weather and system component failure. This is how LPSP is computed [45]:

$$\text{LPSP} = \frac{\sum\left(P_l - P_{pv} - P_{BMG} + P_b + P_{DG}\right)}{\sum P_l} \quad (43)$$

$$\text{AI} = 1 - \text{LPSP} \quad (44)$$

3.4. Objective Function

In order to support the industrial area in Rwamagana, Rwanda, this study objective is to identify the energy system that offers the best overall system performance and economic efficiency for PV/Battery system. The effect of improving the assessment of economic factors like Net Present Cost (NPC) and Cost of Energy (COE) criteria, as well as social factors like Job Creation Opportunity (JCO) and the Human Development Index (HDI), on lowering technical aspects like Loss of Power Supply Probability (LPSP), will also be evaluated. The purpose of this study is to clarify how energy is spread among various setups by looking at excess energy. HDI, JCO, and NPC are additional objective functions that result from system optimisation. Equation (44) can be used to express the optimisation theory

for any system that is being studied [46].

$$\begin{cases} OF_1 = \min\left(\text{NPC}, \text{COE}, \text{LPSP}\right) \\ OF_2 = \max\left(\text{HDI}, \text{JCO}\right) \end{cases} \tag{45}$$

Subject to:

$$\begin{cases} N_x^{\min} \le N_x \le N_x^{\max}, x = \{\text{pv}, \text{Batt}, \text{Storage}, \text{Grid}\} \\ 0 \le \text{LPSP} \le 1\% \end{cases} \tag{46}$$

The number of components that make up the proposed systems is denoted by N_x.

4. Results and Discussion

With an emphasis on technical, economic, environmental, and social aspects, we evaluate the outcomes of the most accurate models of PV/Battery/Grid for grid-connected systems. We focus on this scenario in the analysis as it offers greater reliability, flexibility, and energy independence compared to other setups. The battery allows excess solar energy to be stored during the day and used during peak demand or grid outages, reducing reliance on the utility and mitigating the effects of power interruptions. It also enables better load shifting, allowing users to take advantage of lower electricity prices during off-peak hours and avoid higher tariffs during peak periods. This combination enhances system resilience, optimizes self-consumption, and supports grid stability.

4.1. Optimal Sizing Status Analysis

Figure 7 illustrates the convergence of the PSO algorithm in optimizing load demand for a grid-connected system in the study area.

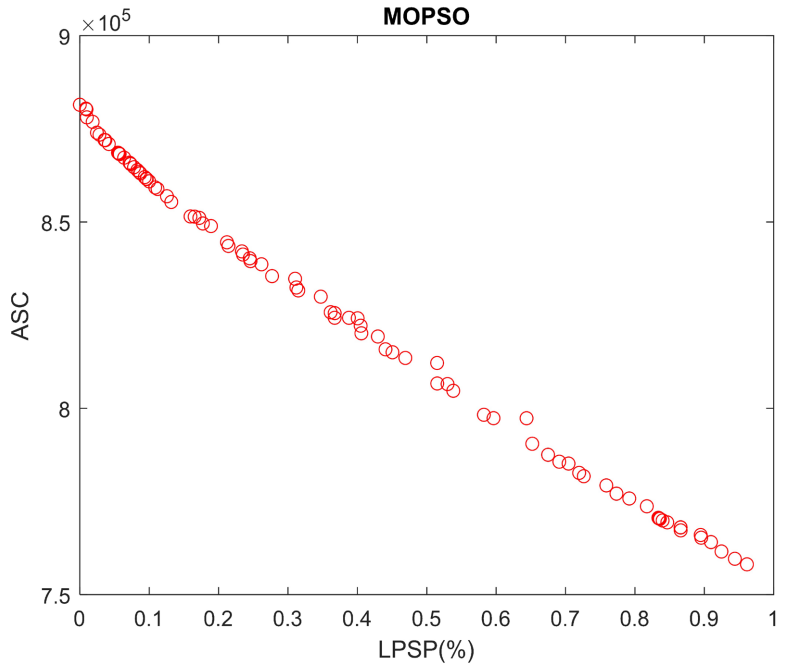

Figure 7. Convergence diagram for the Rwamagana area.

The scatter plot illustrates the relationship between the Loss of Power Supply Probability, (expressed in percentage) and the Annualized System Cost. As observed in Figure 7, there is a clear inverse relationship: as LPSP increases, indicating a higher probability of power supply shortfalls, the ASC decreases. This trend suggests that achieving higher reliability (lower LPSP) comes at a greater financial cost, whereas allowing for more frequent power shortages reduces system expenses. The data points, represented by red open circles, form a relatively smooth downward curve, emphasizing the trade-off between system reliability and cost. This analysis is crucial in designing hybrid renewable energy systems, where decision-makers must balance reliability with economic feasibility.

4.2. Technical, Economic, Environmental, and Social Criteria Results Analysis

In this subtopic, we present a detailed analysis of the technical, economic, environmental and social criteria results obtained from the study as presented in Table 4 on the optimal integration and performance of Rwanda's electrical network with high penetration of interconnected PV rooftop microgrids. By evaluating these criteria, we assess the operational impacts and benefits of widespread PV deployment on the existing grid infrastructure in the study Rwamagana area.

Table 4. Rwamagana optimal sizing of the proposed system.

Solar panels (1 kW)	19,806
Battery units (each 100 kWh)	1820.69
Total solar energy (kWh)	20828448.89
Total energy purchased (kWh)	344711.52
Total energy sold to grid (kWh)	3568803.59
Battery charge energy (kWh)	9451527.89
Battery discharge energy (kWh)	9036620.6
Total Load demand (kWh)	15365172.5
Renewable energy penetration (%)	97.75
Solar PV fraction	96.16
SSSI	0.418
SSCI	0.308
Avoided CO_2 emissions (Kg)	10374932.8
Energy excess	3568803.59
Unmet load	0
HDI	0.326
LPSP	0.00961

4.2.1. Technical Criteria Results Analysis

The obtained technical results demonstrate a well-performing energy system with promising reliability and efficiency indicators, such as SSSI of 0.4186, and SSCI of

0.3088 reflects a reasonable ability of the system to meet energy demands.

These evaluation criteria provide crucial insights into the feasibility, stability, and efficiency of transitioning towards a more decentralized and renewable-powered network in Rwanda and shows the analysis and assessment of best outcomes in the area under study, including the optimum results for technical, economic, and environmental factors.

The system produced an excess energy amount of 3568803.59 kWh, indicating a surplus that could potentially be stored or sold to the grid. Importantly, the unmet load is zero, highlighting that the system successfully met all the required demand without shortages. The LPSP is very low at 0.0096, further emphasizing the system's high reliability. Additionally, the total energy transfer reached 3913515.11 kWh, confirming the system's capability to generate and deliver a substantial amount of energy. Overall, these results suggest a technically strong and reliable energy system with opportunities for optimizing energy excess management.

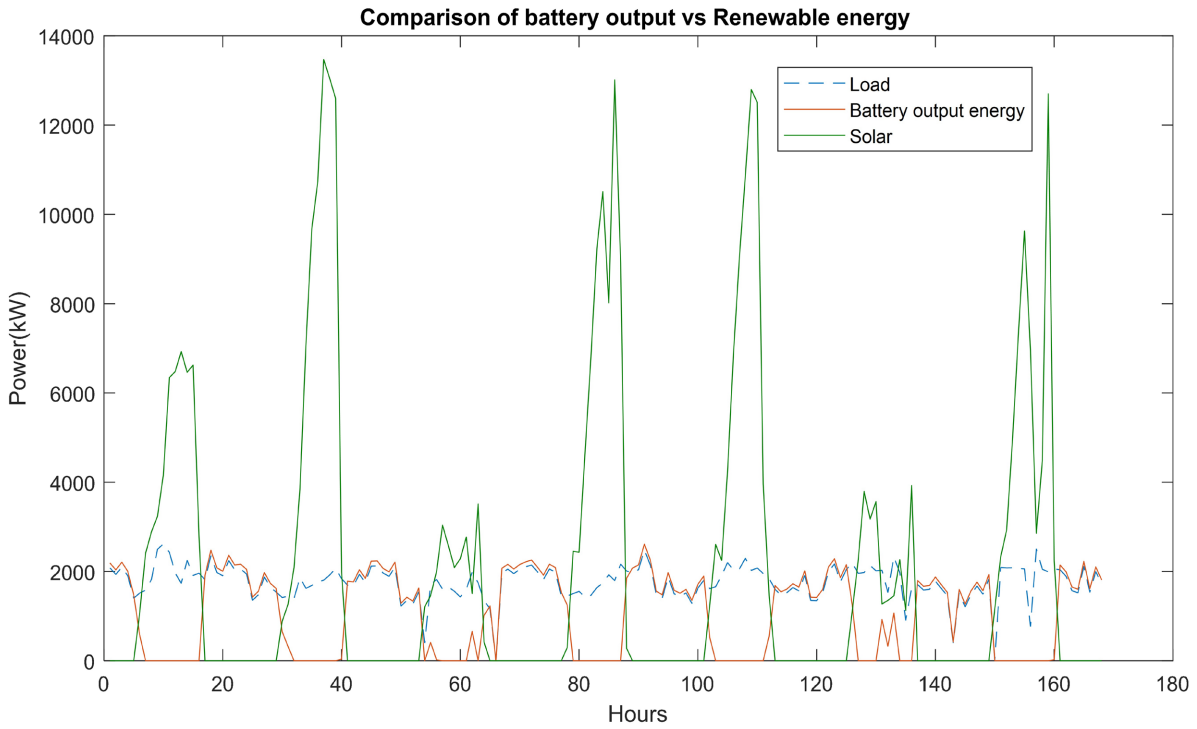

Figure 8. Comparison of the battery and Renewable energy output.

Figure 8 displays the power profiles of system load, battery output energy, and solar generation over approximately 180 hours. The load (blue dashed line) remains relatively stable around 2000 kW, indicating consistent energy demand. Solar power (green line) shows high variability with sharp peaks reaching up to nearly 14,000 kW, highlighting intermittent nature of solar energy input. The battery output (orange line) appears to respond dynamically, providing power during periods of low solar generation and reducing output or charging during high solar availability. This interplay suggests an effective energy management strategy

where the battery compensates for solar fluctuations to ensure a stable power supply that meets the load demand.

Figure 9 illustrates the variation in power over approximately 180 hours, comparing system Load, Battery Charging Load, and Solar Power (SolPower). The dashed blue line represents the constant or mildly fluctuating Load, which remains relatively steady around 2000 kW. In contrast, the red line indicates Battery Charging Load, which shows intermittent charging patterns aligning closely with the availability of solar power. The green line representing SolPower displays a highly variable and peaky profile, with solar generation reaching values above 12,000 kW during sunny intervals. These peaks in SolPower correspond with spikes in Battery Charging Load, demonstrating a strategy of charging batteries primarily when solar energy is abundant, thus enhancing renewable energy utilization.

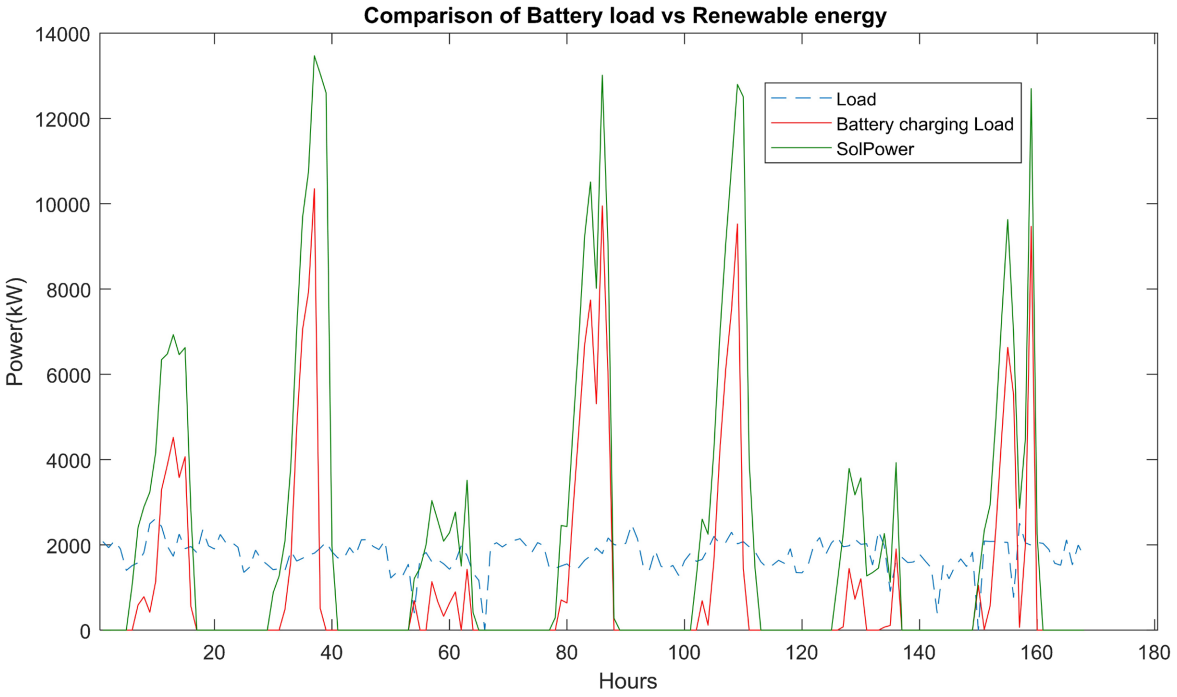

Figure 9. Battery and renewable energy loads comparison.

Figure 10 displays the annual power profile of a battery energy storage system, showing both the charging and discharging behavior over approximately 8760 hours (one year). The blue curve represents battery charging (negative values), indicating power absorption by the battery, while the orange curve represents battery output or discharging (positive values). The sharp and deep fluctuations in the charging curve indicate high variability in energy input, likely due to intermittent renewable sources. Meanwhile, the output remains relatively more stable, although still fluctuating, implying controlled discharge to meet demand or grid support. The data point marker shows a peak charging event at hour 2652 with a power input of approximately −8266.82 kW.

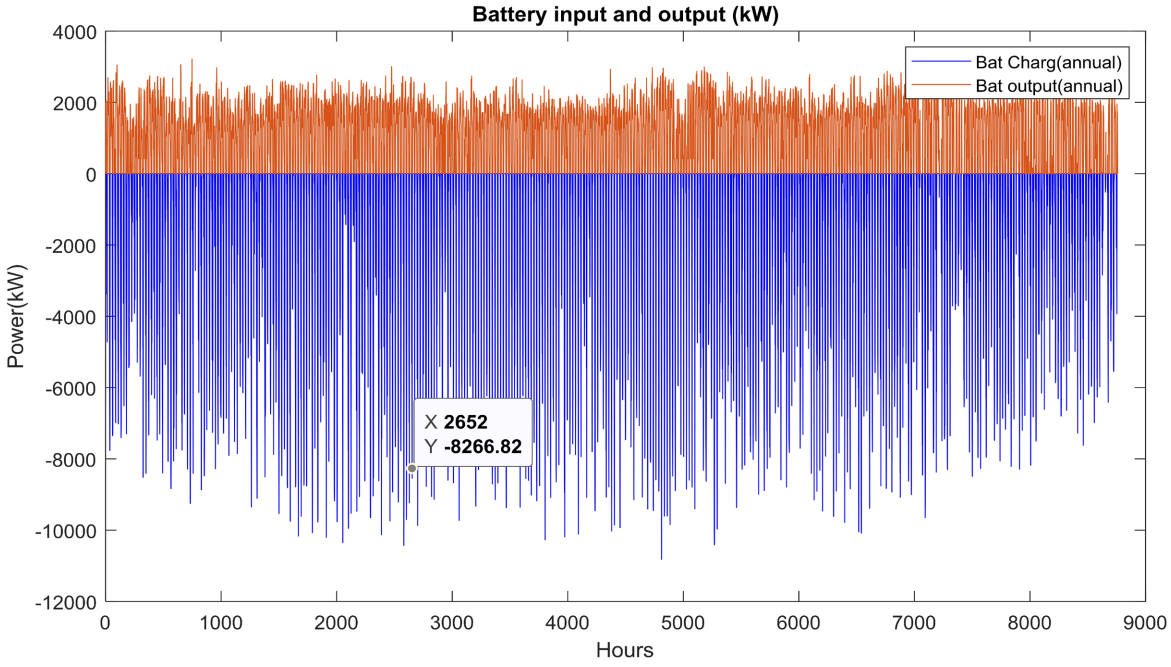

Figure 10. Battery input and output status.

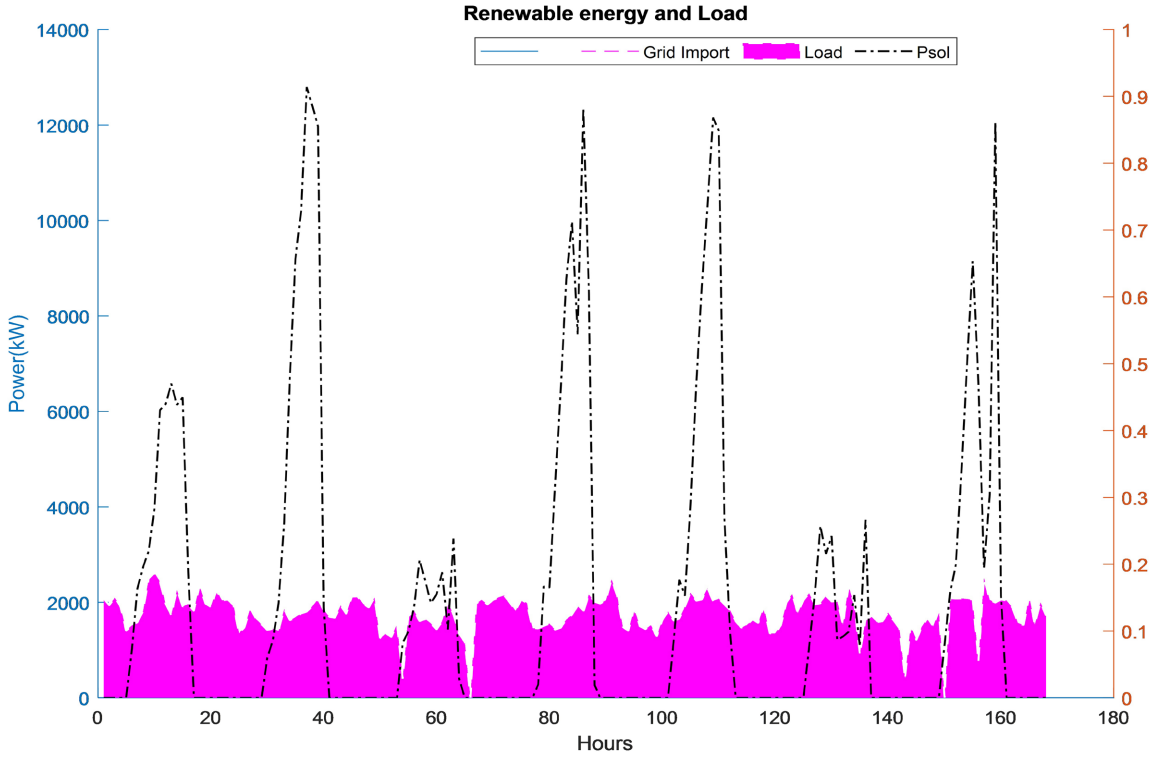

Figure 11. Renewable energy and load.

The chart visualizes the power distribution over time (in hours), highlighting three key parameters: Grid Import, Load, and Solar Power Output (Psol). The left Y-axis (blue) represents power in kilowatts (kW), while the right Y-axis (orange)

corresponds to the normalized scale of solar power output. The magenta-filled area indicates the electrical load, the dashed line shows the Grid Import, and the black dash-dot line represents solar power generation. The plot shows a fluctuating solar output peaking periodically, while the grid import and load remain relatively stable, indicating reliance on grid supply when solar output is insufficient. (Figure 11).

Figure 12 presents the annual power exchange with the grid, showing both grid purchases (blue) and grid sales (orange) across time in hours. The y-axis represents kilowatts (kW) power, while the x-axis spans an entire year (up to 8760 hours). The data illustrates that for the majority of the year, there is a high frequency of grid sales, indicating surplus power, likely from renewable generation such as solar, being exported. Conversely, grid purchases are concentrated in certain periods, likely correlating with times of low renewable generation or high demand. The sporadic and uneven distribution highlights the variability in power flows typical in systems with high renewable energy penetration.

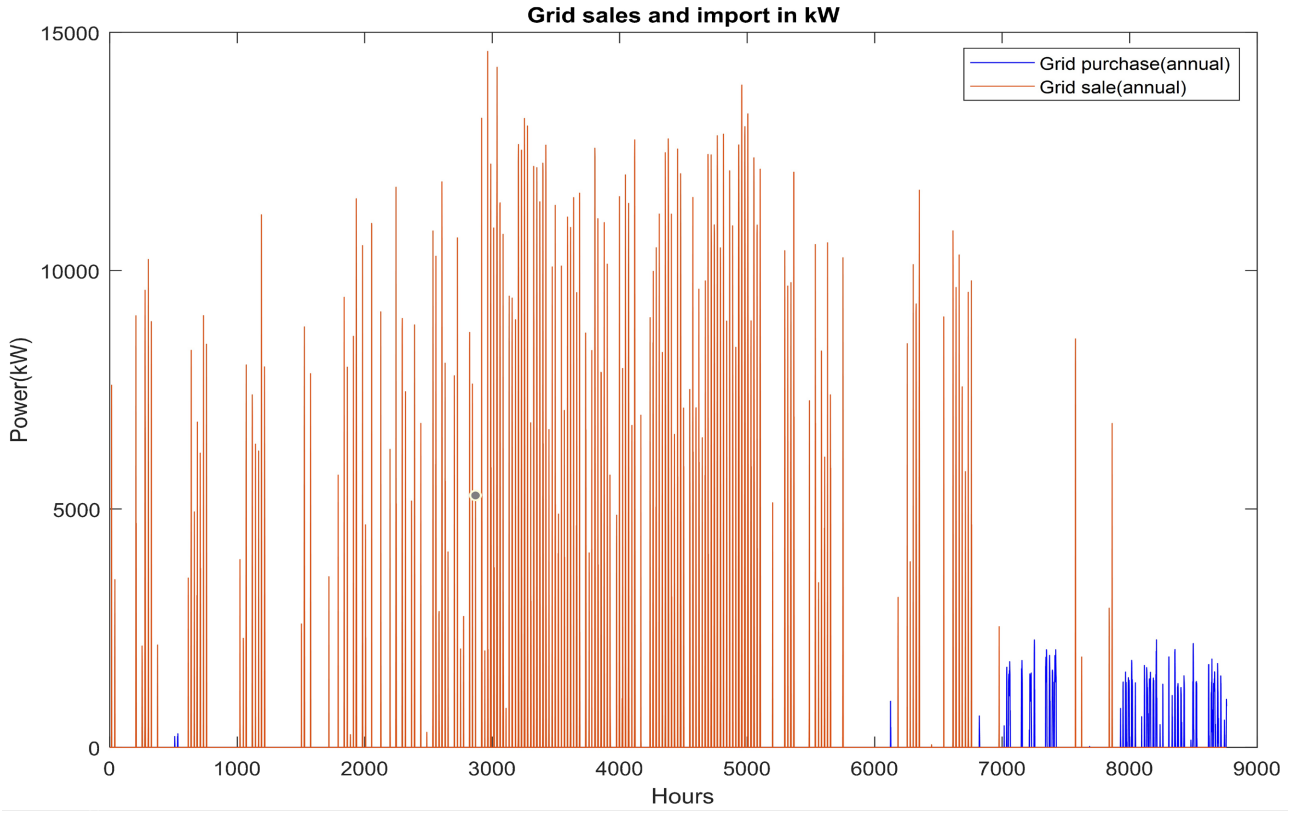

Figure 12. Grid sales and import of studied area.

4.2.2. Economic Criteria Results Analysis

The economic analysis of the system indicates strong financial viability based on the obtained criteria. The LCOE is notably low at 0.04 $/kWh, suggesting cost-effective energy production. The Net Present Cost is calculated at $8867793.27, reflecting the total cost of the project over its lifetime (Table 5).

Table 5. Economic criteria results.

Economic results	Costs ($)
LCOE	0.04
NPC	8867793.27
Payback period	9.6
Annual cost	758129.28
Solar cost	730313.9
Grid cost	−15005.35
Battery cost	41613.49
Inverter cost	1207.24

The payback period is estimated at 9.6 years, meaning the project will recover its initial investment within a reasonable timeframe. The annual operating cost stands at $758129.28, with a significant contribution from solar energy at $730313.90. The grid component contributes a small negative cost of −$15005.35, likely due to energy export revenues or net metering benefits. Battery storage and inverter systems incur additional costs of $41613.49 and $1207.24, respectively. Overall, the results demonstrate that the system is economically attractive, primarily driven by affordable solar energy costs and supported by modest storage and inverter expenses.

The bar chart in Figure 12 illustrates the annualized cost of various energy system components—Battery, Inverter, Solar, and Grid—in USD. It is evident that the Solar component dominates the cost distribution, contributing over $700,000 annually, which likely reflects high initial capital investment and large system size.

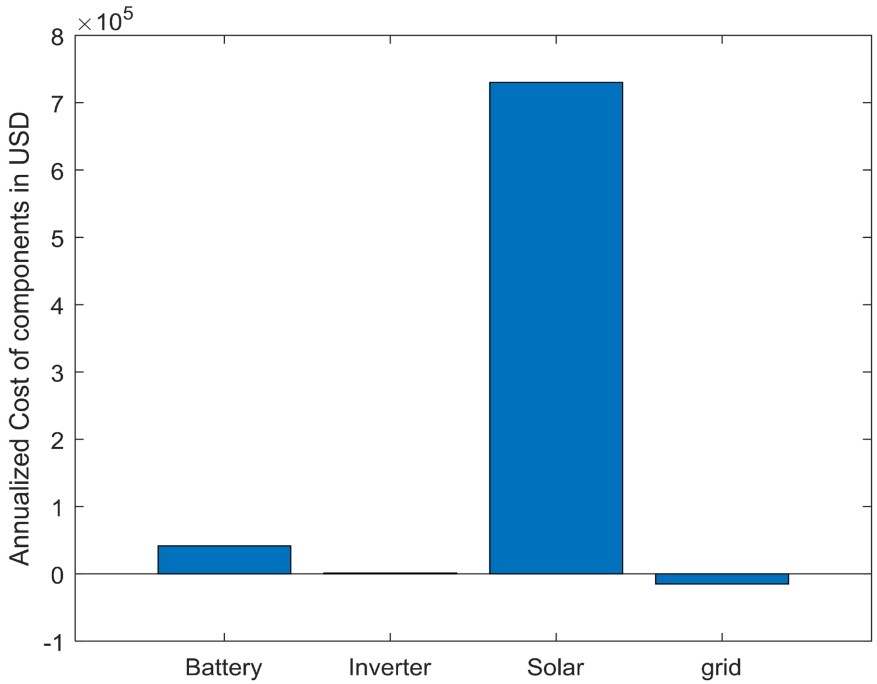

Figure 13. System annual cost for the Rwamagana area.

The Battery system follows, though at a much lower cost, indicating a moderate storage requirement. The Inverter cost is negligible, possibly due to system design or integration efficiencies. Interestingly, the Grid cost appears slightly negative, potentially suggesting revenue from grid exports or avoided grid purchases, highlighting the system's economic interaction with external electricity networks (**Figure 13**).

4.2.3. Environmental Criteria Results Analysis

In this study, the environmental impact was assessed using two key criteria: avoided CO_2 emissions and renewable energy penetration. The results demonstrate a significant positive outcome, with a total of 10374932.8 kilograms of CO_2 emissions avoided, highlighting the substantial reduction in greenhouse gas emissions achieved through the proposed system (**Figure 14**).

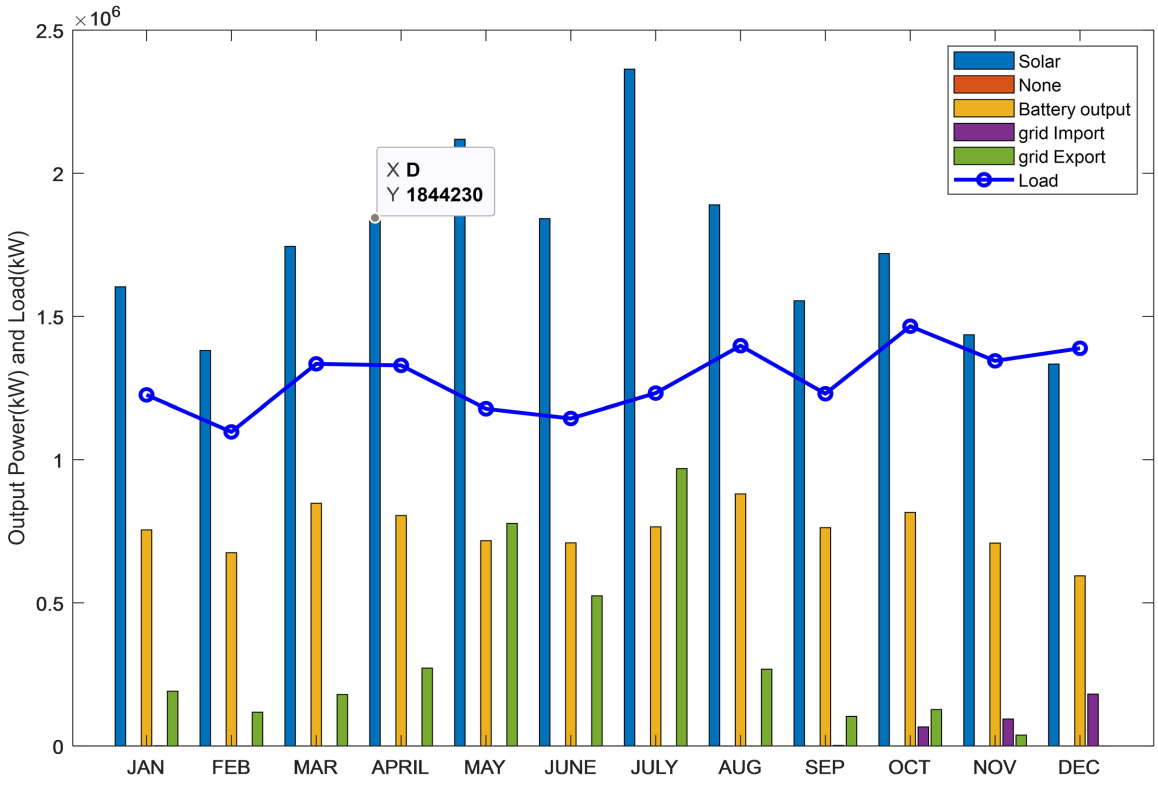

Figure 14. System output power and the load for Rwamagana area.

Furthermore, the renewable energy penetration reached an impressive 97.75%, indicating that nearly the entire energy demand was met through renewable sources. Together, these results underscore the effectiveness of the system in promoting sustainability, reducing reliance on fossil fuels, and contributing meaningfully to climate change mitigation efforts. The monthly energy distribution chart showcases the interplay between various power sources—solar, battery output, and grid (import/export)—and the corresponding load demand throughout the year. Solar energy, represented by the dominant blue bars, consistently con-

tributes the majority of the power, peaking in July due to higher solar irradiance. Battery output and grid import supplement the system, particularly during periods of reduced solar output. Notably, grid export is more prominent in months with excess solar generation, indicating efficient energy utilization and potential economic benefits. The load curve (blue line) remains relatively stable, emphasizing the system's need to adapt to seasonal variations in solar availability.

4.2.4. Social Criteria Results Analysis

The values for the social criteria achieved during the optimization of the proposed systems, using the implemented algorithms, are presented in **Table 3**. In this study, three social criteria were considered: Human Development Index (HDI), job creation opportunities (JCO), and social acceptance. This work is among few studies that assess these social factors within Rwandan context.

Based on simulation results, each system is expected to generate three (3) direct jobs and contribute to improving the HDI. Regarding the third social criterion, social acceptance, we referred to field survey conducted [47] the field survey carried out by on accessibility to renewable energies in SSA and 95% of the surveyed individuals expressed positive attitudes toward adopting or transitioning to RE systems.

5. Conclusion and Future Work

This study has comprehensively analyzed the optimal integration of interconnected rooftop PV microgrids into the Rwandan electrical distribution network, providing valuable insights into technical, economic, social, and environmental dimensions. The simulation results confirm that high penetration of interconnected PV microgrids significantly enhances grid reliability, energy access, and renewable energy adoption. Technically, the system exhibited strong reliability indicators, including a low Loss of Power Supply Probability (0.0096), no unmet load, substantial energy transfer (3913515.11 kWh), and favourable stability indices (SSSI of 0.4186 and SSCI of 0.3088). Economically, the system demonstrated strong viability with a low Levelized Cost of Energy ($0.04/kWh), a reasonable payback period (9.6 years), and acceptable operating costs. Socially, the project supports human development, job creation, and enjoys high social acceptance (95%), while environmentally, it achieved a renewable energy penetration of 97.75% and avoided over 10 million kilograms of CO_2 emissions. Overall, the findings highlight that interconnected rooftop PV microgrids offer a technically feasible, economically viable, socially beneficial, and environmentally sustainable pathway to enhance Rwanda's energy transition. However, successful large-scale deployment will require careful planning, advanced grid control strategies, energy storage integration, and supportive regulatory frameworks to maximize benefits and mitigate associated challenges.

Future work will focus on several critical areas to further strengthen this research. Firstly, dynamic modelling under real-time operational conditions will be undertaken to better assess system behaviour under transient and fault scenarios.

Secondly, the integration of advanced energy management systems (EMS) and demand-side response mechanisms will be explored to optimize energy flow and enhance grid flexibility. Thirdly, an in-depth financial sensitivity analysis considering varying policy incentives, market conditions, and technological cost trends will be conducted. Additionally, future studies will investigate hybrid microgrid configurations incorporating other available renewable sources, such as biomass, to enhance system resilience. Lastly, broader social impacts, including long-term effects on community development and energy equity, will be evaluated to ensure a holistic assessment of microgrid deployment in the Rwandan context.

Acknowledgements

The authors thank The Pan-African University (Pan African University Institute for Basic Sciences, Technology, and Innovation) on behalf of the African Union for providing financial assistance.

Contributions of the Authors

Conceptualisation, methodology, software, validation, formal analysis, investigation, resources, writing (original draft), writing (review & editing), and visualisation are all areas in which **Emmanuel Nisingizwe** shines. **Mahamat Adoum Abdoulaye**: Conceptualisation, methodology, software, validation, formal analysis, investigation, resources, writing (original draft), writing (review & editing), and visualisation. **Cyrus Wekesa Wabuge:** Methodology, Writing-review, Supervision, and Conceptualisation. **Michael J. Saulo:** Methodology, Writing-review, Supervision, and Conceptualisation.

Funding

Through PAUSTI, the African Union (AU) provided funding for this study.

Conflicts of Interest

The authors disclose that they have no known conflicts of interest that would have influenced the research presented in this article.

References

[1] I.E. Agency (2021) World Energy Outlook.

[2] Ang, Y.Q., Berzolla, Z.M. and Reinhart, C.F. (2020) From Concept to Application: A Review of Use Cases in Urban Building Energy Modeling. *Applied Energy*, **279**, Article ID: 115738. https://doi.org/10.1016/j.apenergy.2020.115738

[3] Mulleriyawage, U.G.K. and Shen, W.X. (2020) Optimally Sizing of Battery Energy Storage Capacity by Operational Optimization of Residential PV-Battery Systems: An Australian Household Case Study. *Renewable Energy*, **160**, 852-864. https://doi.org/10.1016/j.renene.2020.07.022

[4] Khezri, R., Mahmoudi, A. and Aki, H. (2022) Optimal Planning of Solar Photovoltaic and Battery Storage Systems for Grid-Connected Residential Sector: Review, Challenges and New Perspectives. *Renewable and Sustainable Energy Reviews*, **153**, Arti-

cle ID: 111763. https://doi.org/10.1016/j.rser.2021.111763

[5] Singh, B. and Kumar, A. (2023) Optimal Energy Management and Feasibility Analysis of Hybrid Renewable Energy Sources with BESS and Impact of Electric Vehicle Load with Demand Response Program. *Energy*, **278**, Article ID: 127867. https://doi.org/10.1016/j.energy.2023.127867

[6] Hakimi, S.M., Hasankhani, A., Shafie-khah, M. and Catalão, J.P.S. (2021) Stochastic Planning of a Multi-Microgrid Considering Integration of Renewable Energy Resources and Real-Time Electricity Market. *Applied Energy*, **298**, Article ID: 117215. https://doi.org/10.1016/j.apenergy.2021.117215

[7] International Energy Agency (2022). Renewable Electricity. In: International Energy Agency, Eds. https://www.iea.org/reports/renewables-2022

[8] Sachs, J., Kroll, C., Lafortune, G., Fuller, G. and Woelm, F. (2022) Sustainable Development Report 2022. Cambridge University Press. https://doi.org/10.1017/9781009210058

[9] Maghami, M.R., Hizam, H., Gomes, C., Radzi, M.A., Rezadad, M.I. and Hajighorbani, S. (2016) Power Loss Due to Soiling on Solar Panel: A Review. *Renewable and Sustainable Energy Reviews*, **59**, 1307-1316. https://doi.org/10.1016/j.rser.2016.01.044

[10] Yazdani, H., Radmehr, M. and Ghorbani, A. (2023) Smart Component Monitoring System Increases the Efficiency of Photovoltaic Plants. *Clean Energy*, **7**, 303-312. https://doi.org/10.1093/ce/zkac071

[11] Bouchekara, H.R.E.H., Shahriar, M.S., Irshad, U.B., Sha'aban, Y.A., Mahmud, M.A.P., Javaid, M.S., *et al.* (2021) Optimal Sizing of Hybrid Photovoltaic/Diesel/Battery Nanogrid Using a Parallel Multiobjective Pso-Based Approach: Application to Desert Camping in Hafr Al-Batin City in Saudi Arabia. *Energy Reports*, **7**, 4360-4375. https://doi.org/10.1016/j.egyr.2021.07.015

[12] Dong, J., Xue, Y., Kuruganti, T., Sharma, I., Nutaro, J., Olama, M., *et al.* (2018) Operational Impacts of High Penetration Solar Power on a Real-World Distribution Feeder. 2018 *IEEE Power & Energy Society Innovative Smart Grid Technologies Conference* (*ISGT*), Washington DC, 19-22 February 2018, 1-5. https://doi.org/10.1109/isgt.2018.8403344

[13] Arif, S., Rabbi, A.E., Ahmed, S.U., Hossain Lipu, M.S., Jamal, T., Aziz, T., *et al.* (2022) Enhancement of Solar PV Hosting Capacity in a Remote Industrial Microgrid: A Methodical Techno-Economic Approach. *Sustainability*, **14**, Article No. 8921. https://doi.org/10.3390/su14148921

[14] Husain, A.A.F., Ahmad Phesal, M.H., Kadir, M.Z.A.A., Ungku Amirulddin, U.A. and Junaidi, A.H.J. (2021) A Decade of Transitioning Malaysia toward a High-Solar PV Energy Penetration Nation. *Sustainability*, **13**, Article No. 9959. https://doi.org/10.3390/su13179959

[15] Li, Y., Wang, C. and Li, G. (2020) A Mini-Review on High-Penetration Renewable Integration into a Smarter Grid. *Frontiers in Energy Research*, **8**, Article No. 84. https://doi.org/10.3389/fenrg.2020.00084

[16] Rahman, S., Saha, S., Islam, S.N., Arif, M.T., Mosadeghy, M., Haque, M.E., *et al.* (2021) Analysis of Power Grid Voltage Stability with High Penetration of Solar PV Systems. *IEEE Transactions on Industry Applications*, **57**, 2245-2257. https://doi.org/10.1109/tia.2021.3066326

[17] Ferdowsi, F., Mehraeen, S. and Upton, G.B. (2020) Assessing Distribution Network Sensitivity to Voltage Rise and Flicker under High Penetration of Behind-the-Meter Solar. *Renewable Energy*, **152**, 1227-1240. https://doi.org/10.1016/j.renene.2019.12.124

[18] Sampath Kumar, D., Gandhi, O., Rodríguez-Gallegos, C.D. and Srinivasan, D. (2020) Review of Power System Impacts at High PV Penetration Part II: Potential Solutions and the Way Forward. *Solar Energy*, **210**, 202-221. https://doi.org/10.1016/j.solener.2020.08.047

[19] Aghamohamadi, M., Mahmoudi, A. and Haque, M.H. (2021) Two-Stage Robust Sizing and Operation Co-Optimization for Residential Pv-Battery Systems Considering the Uncertainty of PV Generation and Load. *IEEE Transactions on Industrial Informatics*, **17**, 1005-1017. https://doi.org/10.1109/tii.2020.2990682

[20] Bandyopadhyay, S., Mouli, G.R.C., Qin, Z., Elizondo, L.R. and Bauer, P. (2020) Techno-Economical Model Based Optimal Sizing of Pv-Battery Systems for Microgrids. *IEEE Transactions on Sustainable Energy*, **11**, 1657-1668. https://doi.org/10.1109/tste.2019.2936129

[21] Koskela, J., Rautiainen, A. and Järventausta, P. (2019) Using Electrical Energy Storage in Residential Buildings—Sizing of Battery and Photovoltaic Panels Based on Electricity Cost Optimization. *Applied Energy*, **239**, 1175-1189. https://doi.org/10.1016/j.apenergy.2019.02.021

[22] Vaziri Rad, M.A., Toopshekan, A., Rahdan, P., Kasaeian, A. and Mahian, O. (2020) A Comprehensive Study of Techno-Economic and Environmental Features of Different Solar Tracking Systems for Residential Photovoltaic Installations. *Renewable and Sustainable Energy Reviews*, **129**, Article ID: 109923. https://doi.org/10.1016/j.rser.2020.109923

[23] Liu, Y., Zhong, Y. and Tang, C. (2023) Optimal Sizing of Photovoltaic/Energy Storage Hybrid Power Systems: Considering Output Characteristics and Uncertainty Factors. *Energies*, **16**, Article 5549. https://doi.org/10.3390/en16145549

[24] Ma, J. and Yuan, X. (2023) Techno-Economic Optimization of Hybrid Solar System with Energy Storage for Increasing the Energy Independence in Green Buildings. *Journal of Energy Storage*, **61**, Article ID: 106642. https://doi.org/10.1016/j.est.2023.106642

[25] Azerefegn, T.M., Bhandari, R. and Ramayya, A.V. (2020) Techno-Economic Analysis of Grid-Integrated Pv/Wind Systems for Electricity Reliability Enhancement in Ethiopian Industrial Park. *Sustainable Cities and Society*, **53**, Article ID: 101915. https://doi.org/10.1016/j.scs.2019.101915

[26] Dawoud, S.M., Lin, X. and Okba, M.I. (2018) Hybrid Renewable Microgrid Optimization Techniques: A Review. *Renewable and Sustainable Energy Reviews*, **82**, 2039-2052. https://doi.org/10.1016/j.rser.2017.08.007

[27] Alshammari, N. and Asumadu, J. (2020) Optimum Unit Sizing of Hybrid Renewable Energy System Utilizing Harmony Search, Jaya and Particle Swarm Optimization Algorithms. *Sustainable Cities and Society*, **60**, Article ID: 102255. https://doi.org/10.1016/j.scs.2020.102255

[28] Das, S. and De, S. (2023) MCDM for Simultaneous Optimum Economy, Investment Risk and Environmental Impact for Distributed Renewable Power: Demonstration with an Indian Village Data. *Energy Conversion and Management*, **277**, Article ID: 116631. https://doi.org/10.1016/j.enconman.2022.116631

[29] Fairuz, A., Faeshol Umam, M., Hasanuzzaman, M., Rahim, N.A. and Mujtaba, I.M. (2023) Modeling and Analysis of Hybrid Solar Water Desalination System for Different Scenarios in Indonesia. *Energy Conversion and Management*, **276**, Article ID: 116475. https://doi.org/10.1016/j.enconman.2022.116475

[30] Khezri, R., Mahmoudi, A. and Haque, M.H. (2020) Optimal Capacity of Solar PV and Battery Storage for Australian Grid-Connected Households. *IEEE Transactions on*

Industry Applications, **56**, 5319-5329. https://doi.org/10.1109/tia.2020.2998668

[31] Khan, F.A., Pal, N. and Saeed, S.H. (2021) Optimization and Sizing of SPV/Wind Hybrid Renewable Energy System: A Techno-Economic and Social Perspective. *Energy*, **233**, Article ID: 121114. https://doi.org/10.1016/j.energy.2021.121114

[32] Premkumar, M., Sowmya, R., Ramakrishnan, C., Jangir, P., Houssein, E.H., Deb, S., *et al.* (2023) An Efficient and Reliable Scheduling Algorithm for Unit Commitment Scheme in Microgrid Systems Using Enhanced Mixed Integer Particle Swarm Optimizer Considering Uncertainties. *Energy Reports*, **9**, 1029-1053. https://doi.org/10.1016/j.egyr.2022.12.024

[33] Mohammed, Q.A., Al-Anbarri, A.K. and Hannun, M.R. (2022) Using Particle Swarm Optimization to Find Optimal Sizing of PV-BS and Diesel Generator. *Journal of Engineering and Sustainable Development*, **25**, 51-59. https://doi.org/10.31272/jeasd.25.3.6

[34] Agajie, T.F., Ali, A., Fopah-Lele, A., Amoussou, I., Khan, B., Velasco, C.L.R., *et al.* (2023) A Comprehensive Review on Techno-Economic Analysis and Optimal Sizing of Hybrid Renewable Energy Sources with Energy Storage Systems. *Energies*, **16**, Article No. 642. https://doi.org/10.3390/en16020642

[35] Lombardi, P., Arendarski, B., Suslov, K., Shamarova, N., Sokolnikova, P., Pantaleo, A.M., *et al.* (2018) A Net-Zero Energy System Solution for Russian Rural Communities. *E3S Web of Conferences*, **69**, Article No. 01013. https://doi.org/10.1051/e3sconf/20186901013

[36] Sokolnikova, P., Lombardi, P., Arendarski, B., Suslov, K., Pantaleo, A.M., Kranhold, M., *et al.* (2020) Net-Zero Multi-Energy Systems for Siberian Rural Communities: A Methodology to Size Thermal and Electric Storage Units. *Renewable Energy*, **155**, 979-989. https://doi.org/10.1016/j.renene.2020.03.011

[37] Ciocia, A., Amato, A., Leo, P.D., Fichera, S., Malgaroli, G., Spertino, F. and Tzanova, S. (2021) Systems: Effect of Grid Limitation and Storage Installation.

[38] Li, J., Liu, P. and Li, Z. (2022) Optimal Design and Techno-Economic Analysis of a Hybrid Renewable Energy System for Off-Grid Power Supply and Hydrogen Production: A Case Study of West China. *Chemical Engineering Research and Design*, **177**, 604-614. https://doi.org/10.1016/j.cherd.2021.11.014

[39] Laour, M., Akel, F., Bendib, D. and Chikh, M. (2018) Residential Microgrid Load Management and Optimal Control in Grid Connected and Islanded Mode. 2018 6*th International Renewable and Sustainable Energy Conference* (*IRSEC*), Rabat, 5-8 December 2018, 1-4. https://doi.org/10.1109/irsec.2018.8702847

[40] Ortega, M., Río, P.D., Ruiz, P., Nijs, W. and Politis, S. (2020) Analysing the Influence of Trade, Technology Learning and Policy on the Employment Prospects of Wind and Solar Energy Deployment: The EU Case. *Renewable and Sustainable Energy Reviews*, **122**, Article ID: 109657. https://doi.org/10.1016/j.rser.2019.109657

[41] Mallikarjun, P., Thulasiraman, S.R.G., Balachandran, P.K. & Zainuri, M.A.A.M. (2025). Economic Energy Optimization in Microgrid with PV/Wind/Battery Integrated Wireless Electric Vehicle Battery Charging System Using Improved Harris Hawk Optimization. *Scientific Reports*, **15**, Article 10028. https://doi.org/10.1038/s41598-025-94285-7

[42] Odou, O.D.T., Bhandari, R. and Adamou, R. (2020) Hybrid Off-Grid Renewable Power System for Sustainable Rural Electrification in Benin. *Renewable Energy*, **145**, 1266-1279. https://doi.org/10.1016/j.renene.2019.06.032

[43] Adoum Abdoulaye, M., Waita, S., Wabuge Wekesa, C. and Mwabora, J.M. (2024)

Optimal Sizing of an Off-Grid and Grid-Connected Hybrid Photovoltaic-Wind System with Battery and Fuel Cell Storage System: A Techno-Economic, Environmental, and Social Assessment. *Applied Energy*, **365**, Article ID: 123201. https://doi.org/10.1016/j.apenergy.2024.123201

[44] Peng, J., Lu, L. and Yang, H. (2013) Review on Life Cycle Assessment of Energy Payback and Greenhouse Gas Emission of Solar Photovoltaic Systems. *Renewable and Sustainable Energy Reviews*, **19**, 255-274. https://doi.org/10.1016/j.rser.2012.11.035

[45] Raghuwanshi, S.S. and Arya, R. (2020) Reliability Evaluation of Stand-Alone Hybrid Photovoltaic Energy System for Rural Healthcare Centre. *Sustainable Energy Technologies and Assessments*, **37**, Article ID: 100624. https://doi.org/10.1016/j.seta.2019.100624

[46] Oluoch, S., Lal, P., Susaeta, A., Mugabo, R., Masozera, M. and Aridi, J. (2022) Public Preferences for Renewable Energy Options: A Choice Experiment in Rwanda. *Frontiers in Climate*, **4**, Article ID: 874753. https://doi.org/10.3389/fclim.2022.874753

[47] Hassane, A.I., Didane, D.H., Tahir, A.M., Hauglustaine, J., Manshoor, B., Batcha, M.F.M., *et al.* (2022) Techno-Economic Feasibility of a Remote PV Mini-Grid Electrification System for Five Localities in Chad. *International Journal of Sustainable Engineering*, **15**, 177-191. https://doi.org/10.1080/19397038.2022.2101707